Journal Pre-proofs

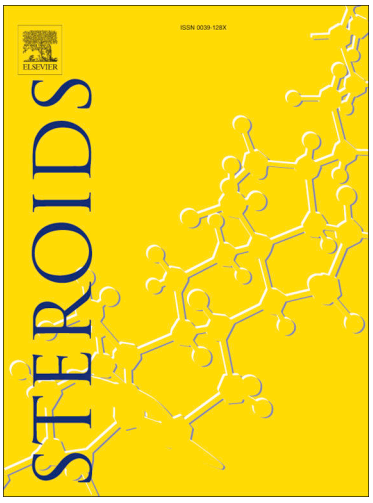

Fabrication of Deoxycholic Acid tethered α-Cyanostilbenes as Smart Low Molecular Weight Gelators and AIEE probes for Bio-imaging

Devesh S. Agarwal, Rajnish Prakash, Prabhat N. Jhad, Rajeev Sakhuja

PII: S0039-128X(20)30084-2
DOI: https://doi.org/10.1016/j.steroids.2020.108659
Reference: STE 108659

To appear in: *Steroids*

Received Date: 11 October 2019
Revised Date: 22 April 2020
Accepted Date: 14 May 2020

Please cite this article as: Agarwal, D.S., Prakash, R., Jhad, P.N., Sakhuja, R., Fabrication of Deoxycholic Acid tethered α-Cyanostilbenes as Smart Low Molecular Weight Gelators and AIEE probes for Bio-imaging, *Steroids* (2020), doi: https://doi.org/10.1016/j.steroids.2020.108659

Fabrication of Deoxycholic Acid tethered α-Cyanostilbenes as Smart Low Molecular Weight Gelators and AIEE probes for Bio-imaging

Devesh S. Agarwal,[a] Rajnish Prakash,[b] Prabhat N. Jha[b] and Rajeev Sakhuja *[a]

[a]*Department of Chemistry, Birla Institute of Technology and Science, Pilani 333 031, Rajasthan, India*

[b]*Department of Biological Sciences, Birla Institute of Technology and Science, Pilani 333 031, Rajasthan, India*

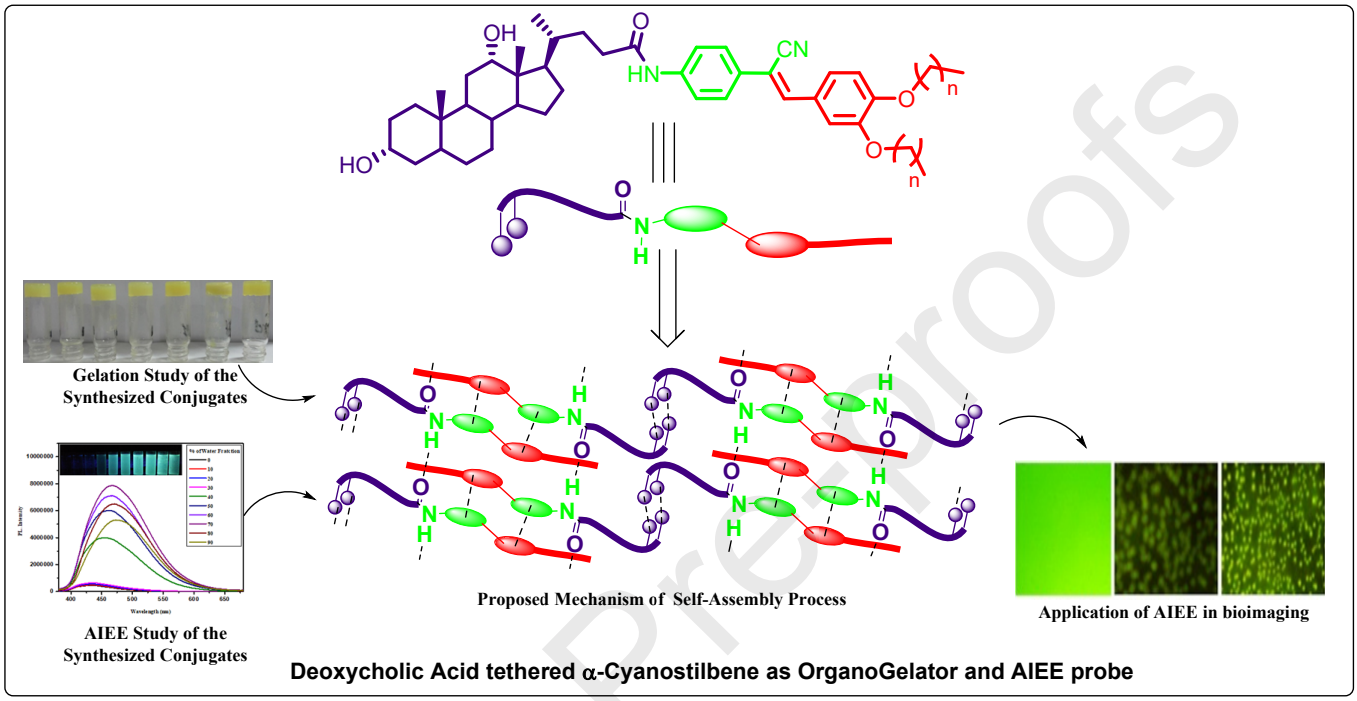

Abstract

Four novel deoxycholic acid tethered *α*-cyanostilbenes were designed, synthesized and characterized using detailed spectroscopic analysis. The synthesized deoxycholic acid tethered *α*-cyanostilbene derivatives formed stable gels with a variety of solvents, such as xylene, toluene, mesitylene, decane, dodecane *etc.* The stable gels showed lamellar sheet type structures stacked over each other, consisting of entangled fibres as evident from SEM, TEM and Fluorescence Microscopy images; The synthesized compounds exhibited AIEE behaviour in H_2O/THF mixture, with the maximum emission observed in 70% H_2O/THF fraction along with a bathochromic shift. A solvent thickening experiment was perform to establish the mechanism of AIEE and the AIEE property was explored for bacterial bio-imaging. The synthesized derivatized steroids proved their potential as multifunctional organic materials.

Keywords: Bile acids; Gelation; AIEE; Bio-imaging

Stilbenes have attracted considerable interest in the past two decades towards investigating their photophysical, photochemical and biological applications.[1-3] Affixing functionalities such as alkyl chain, aromatic/heteroaromatic moieties, donor/acceptor groups and steroidal architectures significantly influence their emission properties in solid and solution states.[4-6] Such functionalized stilbenes have exhibited wide range of applications as self-assembling systems,[7-9] fluorescent probes,[10] liquid crystals,[11] and optoelectronics.[12] Further, the steric effects in α-cyanostilbene plays an important role in the enhancement of emission in aggregation state, while the electronic effects offer great color tunability of AIEE luminogens to widen their emission spectrum.[12-17] Thus, α-cyanostilbenes have been widely studied for their AIEE behaviour,[18-22] and explored for various applications such as bio-imaging,[23,24] analyte detection,[13, 25-27] explosive and biomolecule detection.[28,29]

Strikingly, a few conjugates containing a steroidal moiety appended to α-cyanostilbene have been explored for AIEE and gelation behavior. For example, Kanvah and co-workers studied the AIEE behaviour of the cholesterol appended α-cyanostilbene/diene hybrids (Fig. 1, **I-II**) that exhibited weak emission in organic solvent, however, the emission increased 5-fold accompanied by a strong bathochromic emission shift in aqueous media. In addition, the hybrids exhibited intermolecular charge transfer (ICT) phenomena under aqueous condition in sodium cholate matrix, and the compounds self-assembled to form organized nanostructures having distinct morphologies.[2] Likewise, Zhao and co-workers reported cholesterol appended α-cyanostilbene (Fig. 1, **II**) to be non-fluorescent in assembled state, and found that the emission of free molecules was greatly enhanced upon UV irradiation, which was attributed to the conformational change due to the photo-isomerization of the α-cyanostilbene unit to form capped and branched nanotubes in assembled state. This unique feature has been utilized to detect H_2O_2 with good selectivity and linear response.[30]

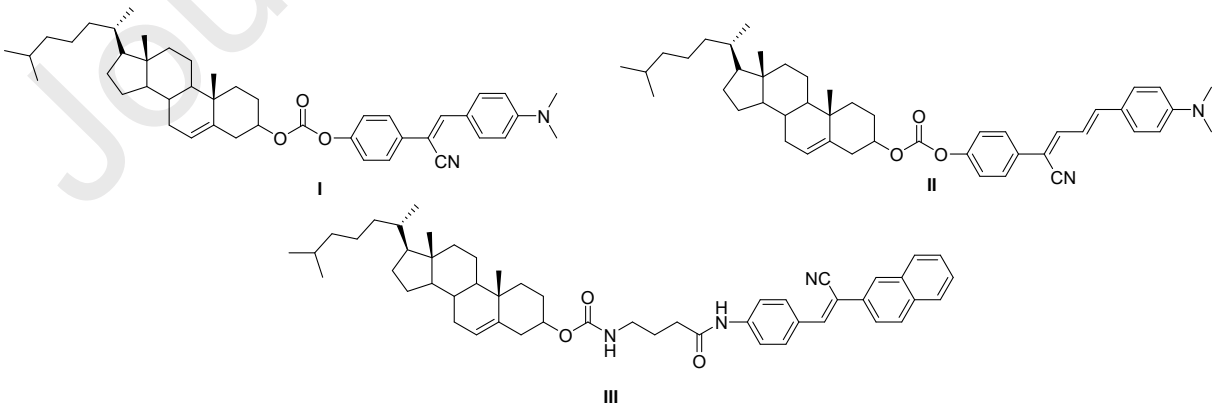

Fig. 1 Previous reported steroid appended α-cyanostilbenes as AIEE probes and organogelator

analogue (Fig. 1, **III**) that formed gels in various aromatic solvents such as xylene, mesitylene, bromobenzene, 2-chlorobenzene, chlorobenzene, 1,2-dichlorobenzene with a CGC of 8.0-15.0 mg/mL. The gels were efficiently used for phase selective gelation of aromatic solvents and absorption of rhodamine dye from water.[31,32] In striking analogy to cholesterol, bile acids are another interesting architectures proven for the self-assembly process, which have been explored towards the formation of organogels and hydrogels with varied applications.[33-36] The presence of hydroxyl groups and a carboxylic acid group on the concave hydrophilic face and methyl groups on the convex hydrophobic face favours the formation of molecular umbrellas or pockets with star-shaped oligomers of bile acids.[37-39] Unfortunately, the development of photo-responsive bile acid appended *α*-cyanostilbene analogues as AIEE probes and organogelators remains unexplored. In continuation to our interest on bile acid based smart materials, [40,41] we plan to affix *α*-cyanostilbene to deoxycholic acid skeleton, and study their AIEE behaviour and gelation.

Results and Discussion

From the outset of the proposed work, the synthesis commenced with the preparation of 3,4-bis(alkyloxy)benzaldehyde (**3a-d**) by *O*-alkylating 3,4-dihydroxybenzaldehyde (**1**) with appropriate bromoalkanes (**2a-d**) in acetone using K_2CO_3 at 65 ºC for 12 h (Scheme 1). Thereafter, **3a-d** on Knoevenagel condensation with 2-(4-nitrophenyl)acetonitrile (**4**) using piperidine in ethanol afforded nitro-substituted bis(alkyloxy) *α*-cyanostilbenes (**5a-d**) in 89-93% yields (Scheme 1). **5a-d** on reduction with stannous chloride in THF/water at 80 ºC furnished their corresponding amino-substituted *α*-cyanostilbenes (**6a-d**) in 80-87% yield. Finally, **6a-d** on coupling with deoxycholic acid (**7**) using EDC.HCl/HOBt/DMAP in DCM afforded DCA tethered bis(alkyloxy) *α*-cyanostilbene hybrids (**8a-d**) in 81-85% yields (Scheme 1). All the intermediates and final compounds were characterized on the basis of ^{1}H NMR, ^{13}C NMR and IR spectroscopy.

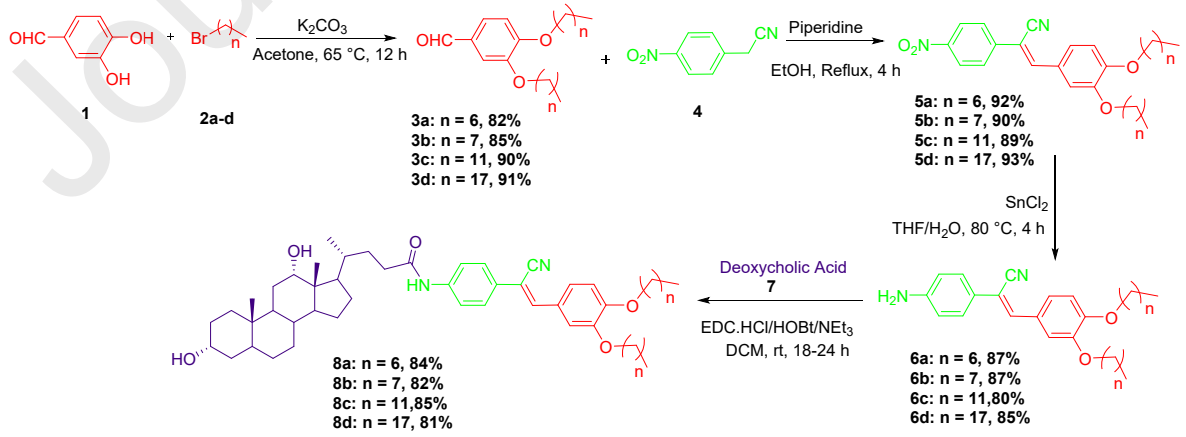

Scheme 1. Systematic route for the synthesis of DCA tethered α-cyanostilbene hybrids (**8a-d**)

The synthesized compounds (**8a-d**) were studied for their gelation behaviour in a variety of solvents using inverted test tube method. To our delight, the synthesized molecules gelate a wide range of solvents including octane, dodecane, decane, tetradecane, hexadecane, toluene, benzene, xylene, mesitylene, iodobenzene, fluorobenzene, decanol, octanol, dimethylformamide (DMF) and dimethyl sulfoxide (DMSO) (Fig. 2: representative gels of **8b** and **8c**). The minimum gel concentration for the compounds varied from 1% to 16% w/v (Table 1).

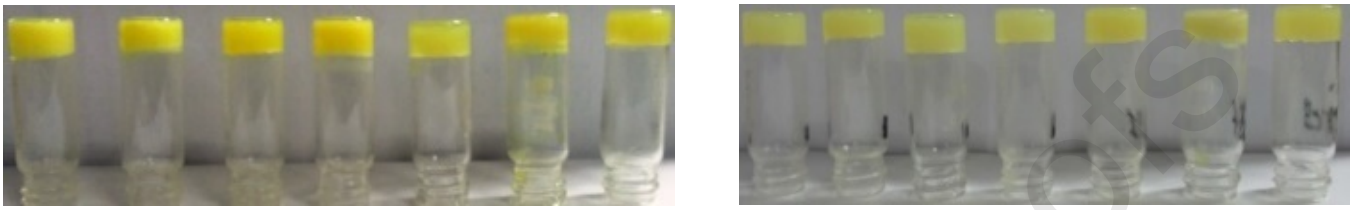

Fig. 2 Inverted vials showing stable gels of **8b** (left) and **8c** (right) in different solvents (left to right: xylene, toluene, mesitylene, decane, dodecane, tetradecane, hexadecane)

Table 1. Gelation studies of **8a**-d in different solvents

Solvent	8a	8b	8c	8d
Xylene	G (1.6)	G (1.4)	G (1)	G (1)
Toluene	G (1.2)	G (1.3)	G (1)	G (1.3)
Mesitylene	G (1.2)	G (1.3)	G (1.1)	G (1.2)
Iodobenzene	G (1.3)	G (1.3)	WG (1.1)	WG (1.4)
Fluorobenzene	G (1.3)	G (1.2)	WG (1.1)	WG (1.4)
p-Cymene	G (1.3)	G (1.2)	WG (1.1)	WG (1.4)
tert-Butylbenzene	G (1.2)	G (1.3)	WG (1.1)	WG (1.2)
Hexane	WG (10)	WG (10)	PS	PS
Heptane	WG (12)	WG (11)	PS	PS
Octane	G (8)	G (7)	PS	PS
Decane	G (7)	G (8)	G (5)	G (5)
Dodecane	G (7)	G (9)	G (6)	G (4)
Teteradecane	G (9)	G (9)	G (4)	G (4)
Hexadecane	G (7)	G (8)	G (5)	G (6)
Dichloromethane	S	S	S	S
Chloroform	S	S	S	S
1,2-Dichloroethane	I	I	I	I
Methanol	PS	PS	PS	PS
Ethanol	PS	PS	PS	PS
isopropanol	PS	PS	PS	PS
tert-Butanol	PS	PS	WG (8)	WG (8)
Decanol	PS	PS	WG (6)	WG (9)
Lauryl alcohol	PS	PS	WG (10)	WG (9)
Acetonitrile	PS	PS	PS	PS
Tetrahydrofuran	S	S	S	S
N,*N*-Dimethylformamide	S	S	WG (16)	WG (14)
Dimethyl sulfoxide	PS	PS	WG (15)	WG (13)

G = gel formed at room temperature [minimum gel concentration (% w/v)]; WG = weak gel (unstable above 20 ºC); PS = partially soluble (a part of it becomes soluble upon heating but re-precipitation was observed after cooling to room temperature); S = soluble; I = insoluble (was not soluble at all even on heating)

To [illegible] on Microscopy (SEM) and Transmission Electron Microscopy (TEM) images of the xerogels of **8c** in benzene, toluene and xylene were obtained. The SEM images of the xerogels revealed lamellar sheets stacked over each other, while the TEM images further indicated the presence of fibres entangled into each other, forming sheets (Fig. 3).

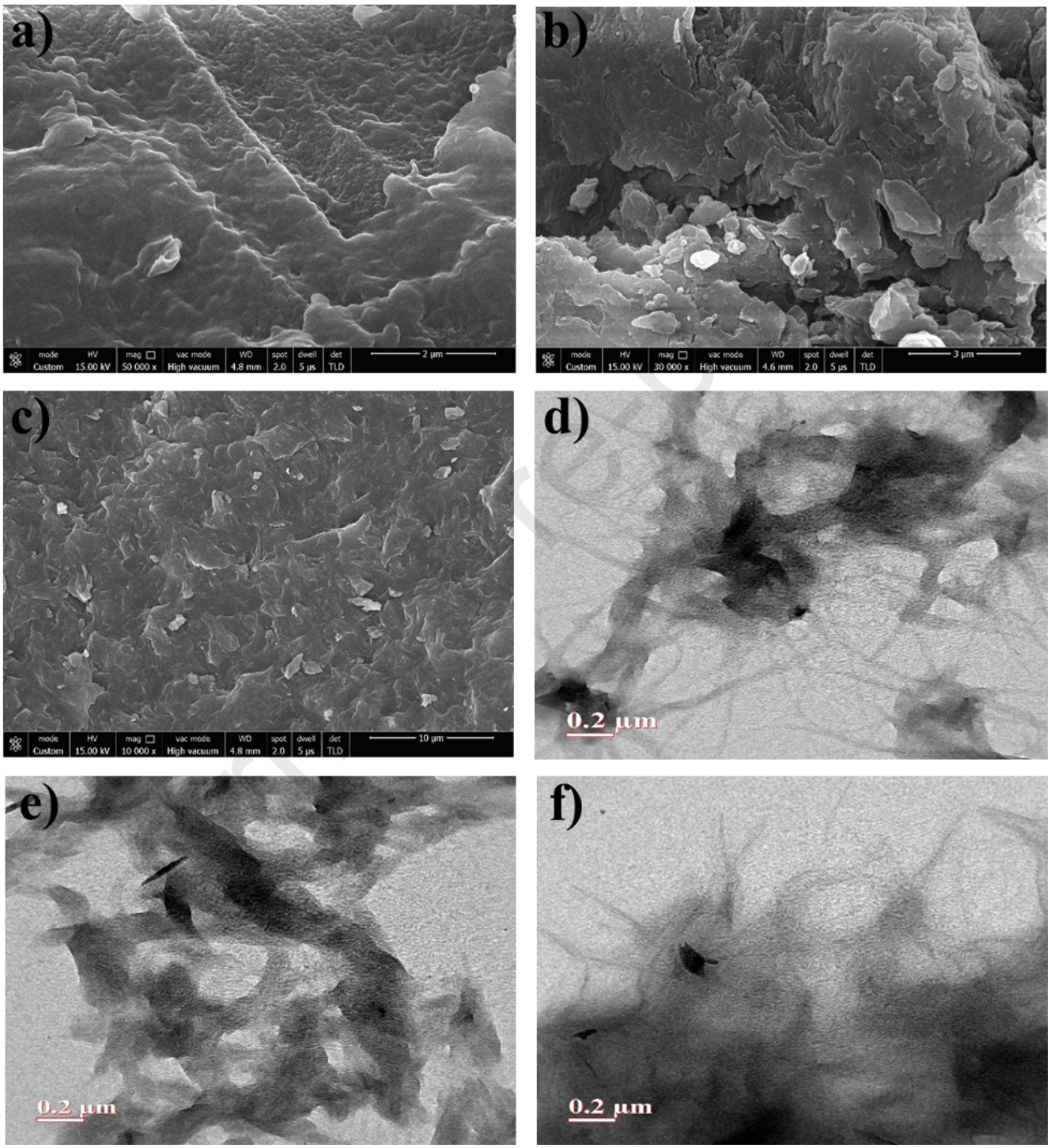

Fig. 3 SEM images of xerogels of **8c** in benzene, toluene and xylene (**a-c**), and TEM images of xerogels of **8c** in benzene, toluene and xylene (**d-f**)

Fl in dodecane**,** while the wet gel of **8c** in toluene revealed a long entangled fibrous network (Fig. 4).

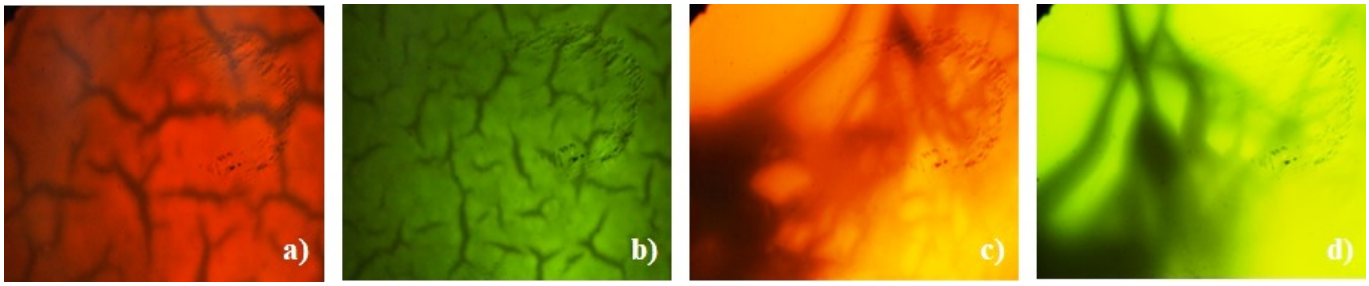

Fig. 4 Fluorescence optical microscopic images of wet gel of **8c** in dodecane (**a-b**) and toluene (**c-d**) in red and green filters

Mechanism of self-assembly process

To get an insight into self-assembly process, FT-IR analysis was performed on the dilute solution of **8c** in DCM, and its xerogel in toluene and decane. The IR spectrum of dilute solution of **8c** in DCM showed prominent bands at 3418 cm^{-1} (O-H/N-H stretching), 2214 cm^{-1} (C≡N stretching), 1666 cm^{-1} (C=O stretching of amide bond) and 1597 cm^{-1} (N-H bending) (Fig. 5). In striking contrast, two well-separated bands at 3448 and 3456 cm^{-1} were observed for the O-H/N-H stretching in the IR spectrum of xerogel of **8c** in toluene (Fig. 5). This indicated the involvement of O-H bond(s) of deoxycholic acid and N-H of amide functionality in hydrogen bonding in the gel state. A red shift in C=O absorption band of amide functionality from 1666 cm^{-1} to 1659 cm^{-1} further supported the above indication. Unfortunately, no change was observed in C≡N stretching of xerogel of **8c** in toluene, and its dilute solution in dichloromethane (DCM). Likewise, in IR spectrum of xerogel of decane, the O-H/N-H overlapped bands were red-shifted to 3474 cm^{-1}, which is in concordance with the above inference of their active contribution in H-bonding (Fig. 5). Contentedly, the two antisymmetric and symmetric stretching vibrations bands of CH_2 appeared at 2924 and 2854 cm^{-1} in the IR spectrum of dilute solution of **8c** in DCM, indicating the possibility of the *gauche* conformation of the two appended *O*-alkyl chains, while in xerogel of **8c** in decane, the band shifted to 2862 cm^{-1} after gelation (Fig. 5). This shift probably suggests indicated the transformation of *gauche* to *trans* conformation of the *O*-alkyl chains to a well-ordered arrangement, restricting their mobility in gel state.

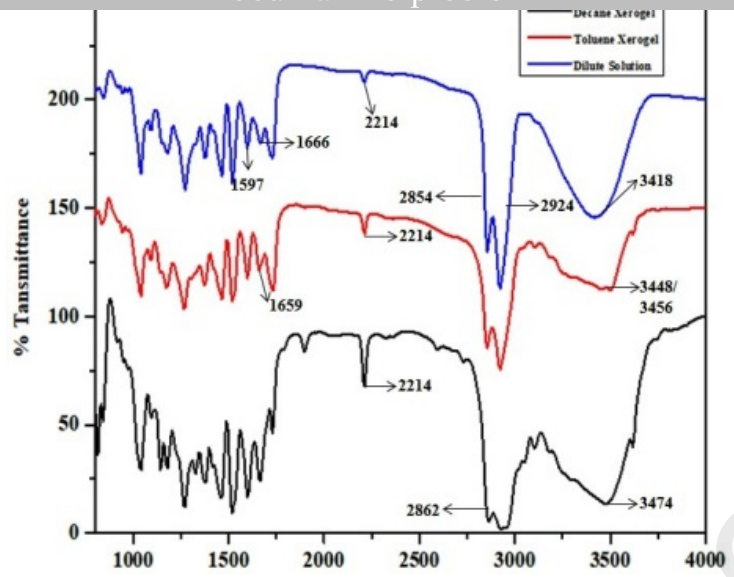

Fig. 5 Comparative FT-IR spectra of **8c** in solution and gel state

It has been well documented that *α*-cyanostilbene undergo *E*- and *Z*- photoisomerization in solution state.[30] To comprehend the impact of affixing deoxycholic acid on the envisioned *E*- and *Z*-photoisomerization of *α*-cyanostilbene in **8**, UV-Visible studies were performed on a sample of **8c** in toluene after irradiating it with UV light (λ = 365 nm) for requisite intervals of time (Fig. 6). As evident from its UV-Visible absorbance spectra, the absorbance band at 365 nm gradually decreased in intensity as well as hypsochromically shifted to 350 nm, with an increase in the exposure time from 0 to 128 minutes. Subsequently, the band at 264 nm gradually increased with a bathochromic shift to 267 nm. The decrease and the increase in the intensity/wavelength of the bands at 365 nm and 264 nm showed an exponential dependence on the irradiation time, which established the phenomena of *E*- and *Z*-photoisomerization in the synthesized conjugate in solution phase (Fig. 6).

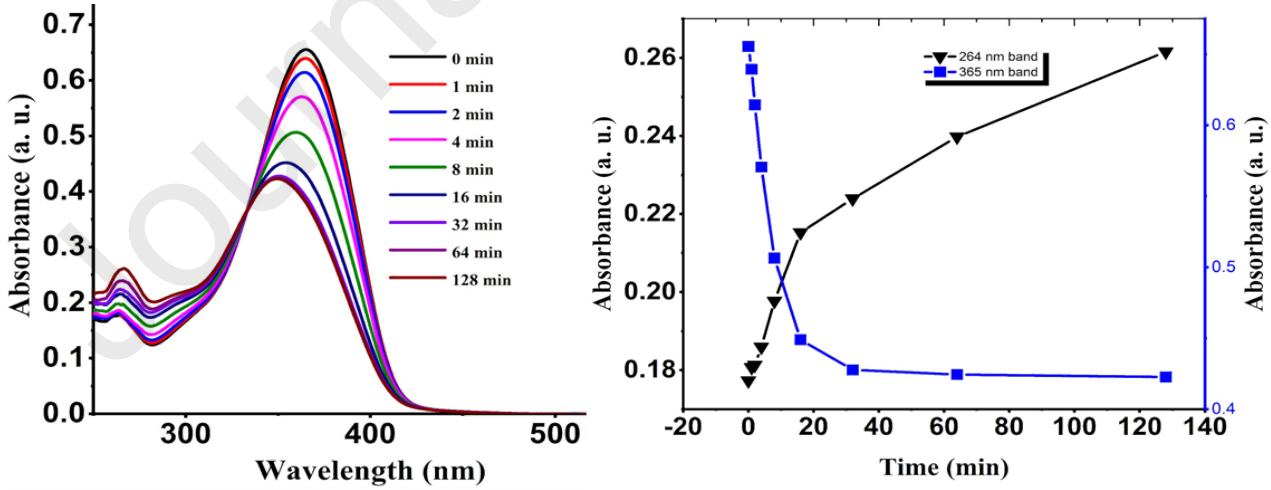

Fig. 6 a) UV-Visible absorption spectra of **8c** after irradiating its dilute solution in toluene with UV-light (λ = 365 nm) at different intervals of time; b) Graph of UV-Visible absorbance bands at 264 nm and 365 nm with irradiation time to indicate the cross-over point

To [illegible] D) analysis of one of the xerogel of **8c** (in toluene) was recorded (Fig. 7). The XRD diffractogram showed a series of intense reflections at 5.44°, 7.42°, 13.28°, 14.78°, 17.18°, 18.74° and 21.82° in the 2θ = 10-30 region, accounting for the corresponding d spacing of 16.2 Å, 11.9 Å, 6.7 Å, 6.0 Å, 5.2 Å, 4.7 Å, 4.2 Å and 3.6 Å, respectively. Among these, the reflection at 3.6 Å can be accounted for the distance between two π-stacked stilbene units in the self-assembled state, while the reflections at 4.7 Å and 4.2 Å accounts for the presence of hydrogen bonded *β* sheet-like arrangement of the gelator molecules in the assembled gel state.[42-45]

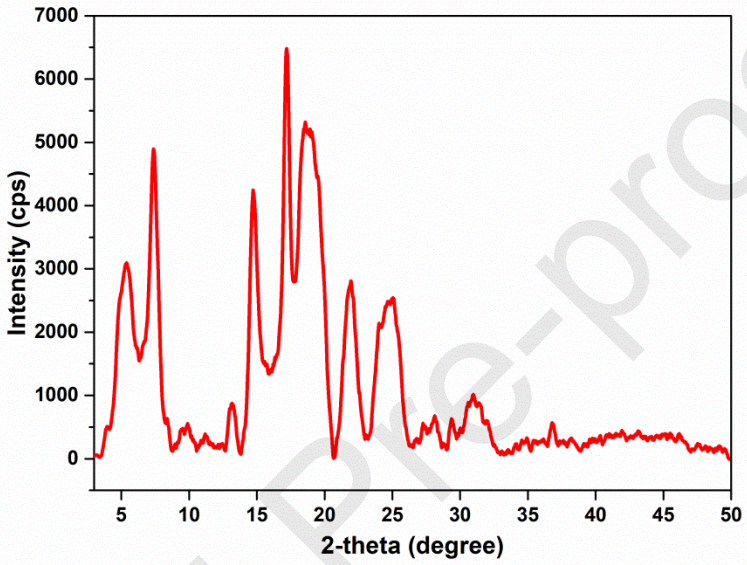

Fig. 7 XRD diffractogram of the xerogel of **8c** in toluene

Based on the FT-IR and XRD studies, it may be concluded that O-H groups of deoxycholic acid play eminent role in strong intermolecular hydrogen bonding, favoring face-to-face amphiphilic packing of deoxycholic acid units leading to elongated fibres. In addition, Z-configuration of *α*-cyanostilbene further provides an additive effect for the $\pi \rightarrow \pi$ stacking between two encountered aromatic clouds. Further, the hydrogen bonding between N-H and C=O groups of the amide bonds between two parallelly-elongated fibrous units may lead to their stacking, resulting in three-dimensional network of lamellar stacked sheets as evident from SEM and TEM images (Fig. 8).[33, 46-49]

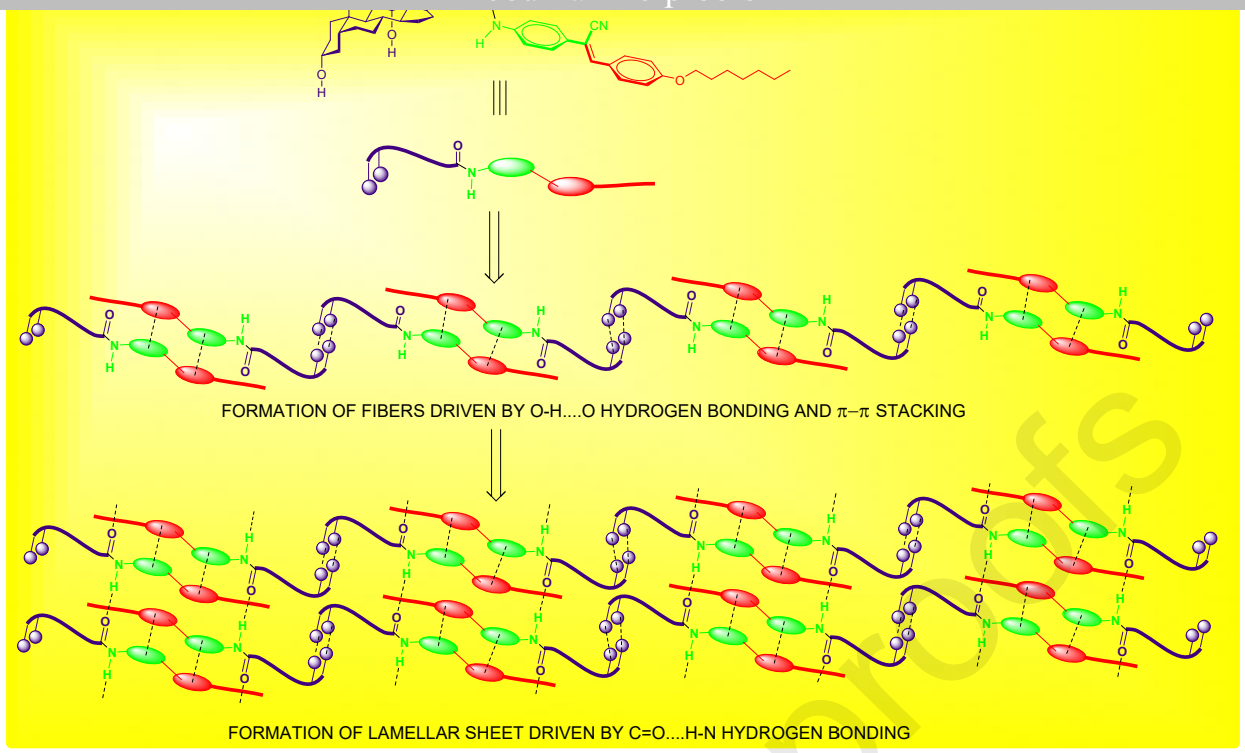

Fig. 8 Plausible mode of aggregation in the self-assembly process

Aggregation-induced emission Enhancement (AIEE) study

α-Cyanostilbenes are known to exhibit enhanced emission in the solid state due to AIEE. Thus, we evaluated the AIEE property in THF/water mixture. In case of **8a**, a significant increase in the photoluminescence was observed on increasing the water fraction from 0% to 70%, however thereafter a slow decrease with further increase in the water concentration was observed. The emission intensity reached a maximum in 70% water/THF fraction, with a bathochromic shift in the wavelength of 37 nm (i.e. from 433 nm to 470 nm) (Fig. 9a). Similar results were observed for **8b**, where a bathochromic shift of 27 nm was evident from 433 nm to 460 nm (Fig. 9b). Likewise, in case of **8c** and **8d**, bathochromic shifts of 35 nm and 34 nm, and significant increase in the photoluminescence intensity were observed on increasing the water fraction from 0% to 70%, respectively (Fig. 9c-d). Such drastic shifts in the emission could be attributed to the formation of aggregated species that results in the confinement of the molecular motion. This structural rigidity further results in enhanced radiative transitions.

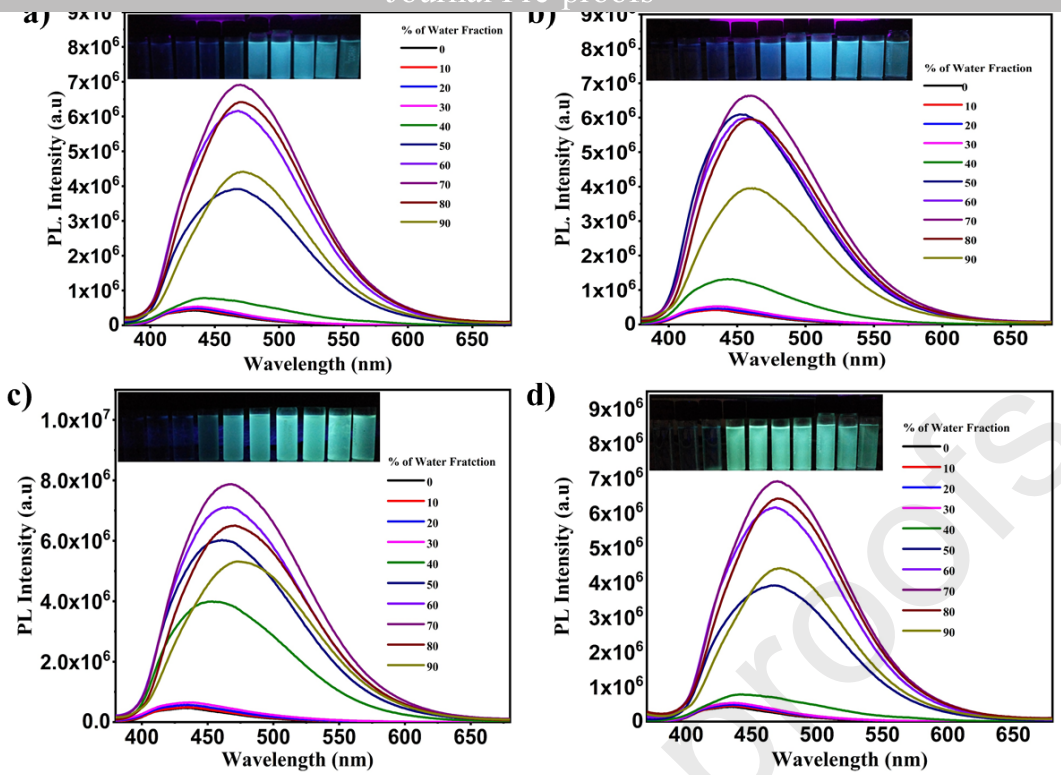

Fig. 9 Photoluminescence intensity spectra of **24a-d** in varying water/THF fraction (a-d) (Inset: Picture showing the enhancement in PL intensity in increasing the water fraction from 0 to 90% from left to right)

To further verify the enhancement emission is due to aggregation, solid state emission spectra of synthesized compounds (**8a-d**) were recorded (Fig. 10). The bands in the emission spectra of **8a-d** in solid state were narrower and of high intensity as compared to that in 70% water/THF fraction, as elucidated from their full width half maxima calculations (Table 2). This could be due to reduced intermolecular molecular rotations and packing efficiency as earlier documented by others.

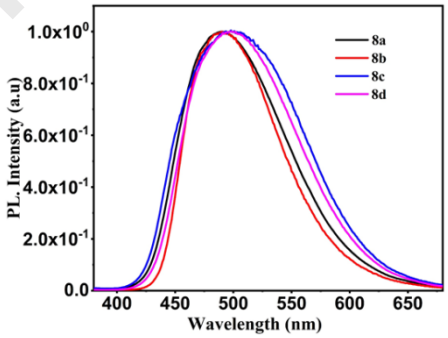

Fig. 10 Solid photoluminescence spectra of **8a-d**

Ta

Compound	Emission in 70% water/THF state (nm)	Emission in solid state (nm)
8a	470	490
8b	460	490
8c	468	498
8d	467	498

To further support the AIEE, solution thickening experiment was carried out for **8c** as a representative example using PEG/THF mixture, as PEG is favorable for increasing the viscosity of the mixture. Interestingly, on increasing the amount of PEG from 0 to 90%, an enhancement in the emission band was observed, and the maximum emission was observed in 90% PEG fraction (Fig. 11). Clearly, the emission intensity significantly enhanced on increasing the viscosity of the solvent mixture probably due to restriction of intermolecular rotation (RIR), thus giving an evidence for the AIEE property of the compound.

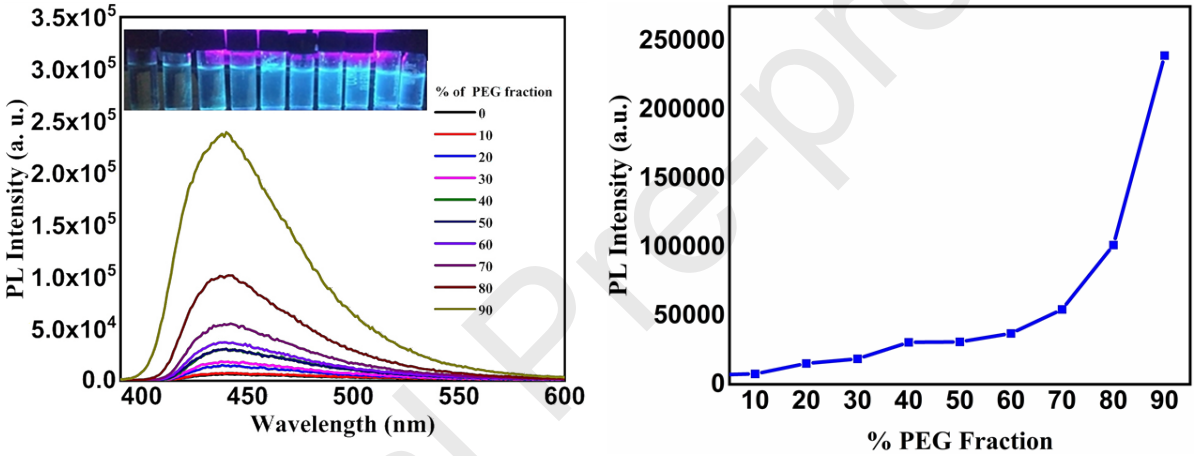

Fig. 11 a) Photoluminescence intensity graph of **8c** in varying PEG/THF fraction (Inset: Picture showing the enhancement in PL intensity in increasing the PEG fraction from 0 to 90% from left to right.); b) Graph of photoluminescence intensity ($\lambda_{Ex.}$ = 365 nm) and PEG fraction

Application of AIEE property

In order to explore their application in the imaging of living cells, the synthesized compounds (**8a-d**) were evaluated for their ability to stain the broad spectrum (gram +ve & gram –ve) bacterial cells (Fig. 12). It became evident that the treatment of bacterial cells showed strong fluorescence behavior. The staining ability of the compounds could be due to their ability to penetrate the bacterial cell membrane. Using a Fluorescence Microscope, it was obvious that the bacteria displayed bright fluorescence in the green channel (530–590 nm). Therefore, the resent observation clearly supports the ability of the compounds as fluorescent probes for staining the broad spectrum bacteria.

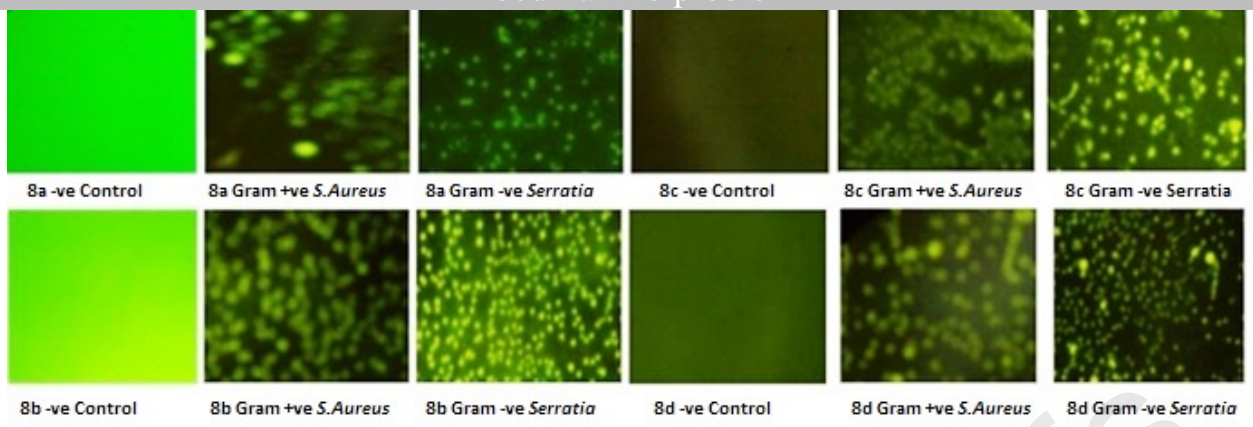

Fig. 12 Fluorescence images of gram +ve (*S. Aureus*) and gram –ve (*Serratia*) with compounds **24a-d** images in the green channel. The scale bar is 10 μM

Conclusion

In summary, we have successfully synthesized deoxycholic acid tethered α-cyanostilbene derivatives as multifunctional materials. All the synthesized compounds were characterized using detailed spectroscopic analysis. The synthesized deoxycholic acid tethered α-cyanostilbene derivatives formed stable gels with a variety of solvents, such as xylene, toluene, mesitylene, decane, dodecane etc. The morphology of the formed gels were in detailed characterized using SEM, TEM and Fluorescence Microscopy that showed lamellar sheet type structures stacked over each other, consisting of entangled fibres. The synthesized compounds also exhibited AIEE behaviour in Water/THF mixture. The maximum emission was observed in 70% water/THF fraction with a bathochromic shift, and a solvent thickening experiment was carried out to establish the mechanism of AIEE. The AIEE property of the hybrids was finally used for bacterial bio-imaging, which established the multifunctional behavior of the synthesized organic materials.

Experimental

General materials and methods

All the chemicals were purchased from Sigma-Aldrich, Alfa Aesar, and Spectrochem India Pvt. Ltd and used without further purification. The solvents used were purchased from Merck (India) and were distilled and dried before use. Nuclear magnetic resonance spectra were recorded on Bruker 400 spectrometer. The ^{1}H NMR experiments were reported in δ units, parts per million (ppm), and were measured relative to residual chloroform (7.26 ppm) or DMSO (2.5 ppm) in the deuterated solvent. The ^{13}C NMR spectra were reported in ppm relative to deuterochloroform (77.0 ppm) or DMSO-d_6 (39.5 ppm). All coupling constants J were reported in Hz. The following abbreviations were used to describe peak splitting patterns when appropriate: s = singlet, d = doublet, t = triplet, dd = doublet of doublet, m = multiplet and brs = broad singlet. Melting points were determined on a capillary point apparatus equipped with a digital thermometer and are

un m silica gel F254 plates (Merck). High resolution mass spectra were recorded on an Agilent Technologies 6545 Q-TOF LC/MS by using electrospray mode.

General procedure for the synthesis of 3,4-bis(alkyloxy)benzaldehydes 4a-d

To a stirred solution of 3,4-dihydroxybenzaldehyde (**1**) (1 mmol) in acetone (20 mL), K_2CO_3 (5 mmol) and appropriate bromo-alkane (**2a-d**) was added. The reaction mixture was refluxed for 12 h and the completion of the reaction was monitored by TLC. After completion, the solvent was removed under reduced pressure, and subsequently water (100 mL) was added, and extracted using ethyl acetate (100 mL x 2). The organic layer was dried over sodium sulphate and concentrated under reduced to give crude product (**3a-d**), which was used for next step without further purification.

General procedure for the synthesis of nitro-substituted bis(alkyloxy) *α*-cyanostilbenes 5a-d

To a stirred solution of 2-(4-nitrophenyl)acetonitrile (**4**) (1 mmol) in hot ethanol (20 mL), 3,4-bis(alkyloxy)benzaldehyde (**3a-d**) (1 mmol) was added. After the reaction mixture became a clear solution, a catalytic amount of piperidine (4 drops) was added, and the reaction turned dark red. The reaction mixture was refluxed for 4 h and the completion of the reaction was monitored by TLC. After the completion, the resultant precipitate was filtered to obtain crude product, which was recrystallized using ethanol to obtain pure **5a-d**.

(*Z*)-3-(3,4-Bis(heptyloxy)phenyl)-2-(4-nitrophenyl)acrylonitrile (5a): Yellow solid; yield: 92% (2.62 g); mp: 97-98 °C; ^{1}H NMR (400 MHz, $CDCl_3$) δ 8.31 (d, J = 8.9 Hz, 2H, H_{Ar}), 7.84 (d, J = 8.9 Hz, 2H, H_{Ar}), 7.75 (d, J = 2.1 Hz, 1H, H_{Ar}), 7.60 (s, 1H), 7.43 (dd, J = 8.4, 2.0 Hz, 1H, H_{Ar}), 6.96 (d, J = 8.5 Hz, 1H, H_{Ar}), 4.11 (dd, J = 11.3, 6.5 Hz, 4H, 2xO-$CH_{2\ Alkoxy}$), 1.93 – 1.85 (m, 4H, 2xO-β-$CH_{2\ Alkoxy}$), 1.56 – 1.47 (m, 4H, 2x$CH_{2\ Alkoxy}$), 1.44 – 1.28 (m, 12H, 2x$CH_{2\ Alkoxy}$), 0.96 – 0.85 (m, 6H, 2xMe_{Alkoxy}); ^{13}C NMR (100 MHz, $CDCl_3$) δ 152.5, 149.1, 147.4, 145.5, 141.2, 126.3, 125.7, 125.5, 124.3, 118.0, 113.0, 112.5, 105.7, 69.3, 69.1, 31.8, 31.8, 29.1, 29.1, 29.1, 26.0, 25.9, 22.6, 14.1; IR (KBr, $\bar{\upsilon}$, cm^{-1}) 2924, 2854, 2206, 1582, 1512, 1111, 849.

(*Z*)-3-(3,4-Bis(octyloxy)phenyl)-2-(4-nitrophenyl)acrylonitrile (5b): Yellow solid; yield: 90% (2.51 g); mp: 99-100 °C; ^{1}H NMR (400 MHz, $CDCl_3$) δ 8.32 (d, J = 8.9 Hz, 2H, H_{Ar}), 7.84 (d, J = 8.9 Hz, 2H, H_{Ar}), 7.74 (d, J = 1.9 Hz, 1H, H_{Ar}), 7.60 (s, 1H, =CH), 7.43 (dd, J = 8.4, 1.9 Hz, 1H, H_{Ar}), 6.96 (d, J = 8.5 Hz, 1H, H_{Ar}), 4.11 (dd, J = 11.3, 6.5 Hz, 4H, 2xO-$CH_{2\ Alkoxy}$), 1.93 – 1.83 (m, 4H, 2xO-β-$CH_{2\ Alkoxy}$), 1.56 – 1.47 (m, 4H, 2x$CH_{2\ Alkoxy}$), 1.42 – 1.27 (m, 16H, 2x$CH_{2\ Alkoxy}$), 0.96 – 0.87 (m, 6H, 2xMe_{Alkoxy}); ^{13}C NMR (100 MHz, $CDCl_3$); 152.5, 149.1, 147.4, 145.5, 141.3, 126.3, 125.7, 125.5, 124.4, 119.0, 113.1, 112.5, 105.7, 69.3, 69.1, 31.8, 29.4, 29.4, 29.3, 29.3,

1142, 843.

(*Z*)-3-(3,4-Bis(dodecyloxy)phenyl)-2-(4-nitrophenyl)acrylonitrile (5c): Yellow solid; yield: 89% (2.32 g); mp: 104-105 °C; ^{1}H NMR (400 MHz, $CDCl_3$) δ 8.32 (d, J = 8.9 Hz, 2H, H_{Ar}), 7.84 (d, J = 9.0 Hz, 2H, H_{Ar}), 7.74 (d, J = 2.1 Hz, 1H, H_{Ar}), 7.60 (s, 1H, =CH), 7.43 (dd, J = 8.5, 2.0 Hz, 1H, H_{Ar}), 6.96 (d, J = 8.5 Hz, 1H, H_{Ar}), 4.11 (dd, J = 11.3, 6.5 Hz, 4H, 2xO-$CH_{2\ Alkoxy}$), 1.93 – 1.84 (m, 4H, 2xO-β-$CH_{2\ Alkoxy}$), 1.55 – 1.47 (m, 4H, 2x$CH_{2\ Alkoxy}$), 1.40 – 1.24 (m, 32H, 2x$CH_{2\ Alkoxy}$), 0.95 – 0.86 (m, 6H, 2xMe_{Alkoxy}); ^{13}C NMR (100 MHz, $CDCl_3$) δ 152.5, 149.1, 147.4, 145.5, 141.3, 126.3, 125.7, 125.5, 124.3, 118.0, 113.1, 112.5, 105.7, 69.3, 69.1, 32.0, 29.7, 29.7, 29.7, 29.7, 29.6, 29.4, 29.4, 29.1, 29.0, 26.0, 26.0, 22.7, 14.1; IR (KBr, $\bar{\upsilon}$, cm^{-1}) 2916, 2847, 2206, 1582, 1512, 1111, 856.

(*Z*)-3-(3,4-bis(octadecyloxy)phenyl)-2-(4-nitrophenyl)acrylonitrile (5d): Yellow solid; yield: 93% (2.26 g); mp: 115-116 °C; ^{1}H NMR (400 MHz, $CDCl_3$) δ 8.32 (d, J = 8.9 Hz, 2H, H_{Ar}), 7.84 (d, J = 8.8 Hz, 2H, H_{Ar}), 7.75 (d, J = 2.0 Hz, 1H, H_{Ar}), 7.60 (s, 1H, =CH), 7.43 (dd, J = 8.4, 2.0 Hz, 1H, H_{Ar}), 6.96 (d, J = 8.5 Hz, 1H, H_{Ar}), 4.11 (dd, J = 11.4, 6.4 Hz, 4H, 2xO-$CH_{2\ Alkoxy}$), 1.92 – 1.85 (m, 4H, 2xO-β-$CH_{2\ Alkoxy}$), 1.54 – 1.47 (m, 2x$CH_{2\ Alkoxy}$), 1.41 – 1.18 (s, 56H, 2x$CH_{2\ Alkoxy}$), 0.90 (t, J = 6.8 Hz, 6H, 2xMe_{Alkoxy}); ^{13}C NMR (100 MHz, $CDCl_3$) δ 152.5, 149.1, 147.4, 145.5, 141.3, 126.3, 125.7, 125.5, 124.3, 118.0, 113.1, 112.5, 105.7, 69.3, 69.1, 32.0, 29.7, 29.7, 29.7, 29.6, 29.4, 29.4, 29.1, 29.0, 26.0, 26.0, 22.7, 14.2; IR (KBr, $\bar{\upsilon}$, cm^{-1}) 2916, 2854, 2206, 1582, 1512, 1342, 1281, 1011, 849.

General procedure for the synthesis of amino-substituted *α*-cyanostilbenes 6a-d

To a stirred solution of **5a-d** (1.89 mmol) in THF/H_2O (20 mL : 5mL), $SnCl_2$ (5.67 mmol) was added and the reaction mixture was refluxed for 4 h. The completion of the reaction was monitored by TLC. After the completion, the reaction mixture was cooled to 0 °C and the pH was adjusted to 10 using saturated solution of sodium bicarbonate (30 mL). Subsequently, ethyl acetate (20 mL) was added, and the reaction was filtered through celite and the organic layer was separated. The organic layer was dried over sodium sulphate and concentrated under reduced to give crude product, which was recrystallized using ethyl acetate/hexanes to give pure product **6a-d**.

(*Z*)-2-(4-Aminophenyl)-3-(3,4-bis(heptyloxy)phenyl)acrylonitrile (6a): Yellow solid; yield: 87% (1.63 g); mp: 113-114 °C; ^{1}H NMR (400 MHz, $CDCl_3$) ^{1}H NMR (400 MHz, $CDCl_3$) δ 7.62 (d, J = 2.0 Hz, 1H, H_{Ar}), 7.48 (d, J = 8.6 Hz, 2H, H_{Ar}), 7.32 (dd, J = 8.4, 2.0 Hz, 1H, H_{Ar}), 7.29 (s, 1H), 6.91 (d, J = 8.4 Hz, 1H, H_{Ar}), 6.74 (d, J = 8.6 Hz, 2H, H_{Ar}), 4.14 – 4.03 (m, 4H, 2xO-$CH_{2\ Alkoxy}$), 3.88 (brs, 2H, NH_2), 1.92 – 1.82 (m, 4H, 2xO-β-$CH_{2\ Alkoxy}$), 1.56 – 1.46 (m, 4H, 2xCH_{2}

Alkoxy)[illegible] (2-Alkoxy)[illegible] Alkoxy)[illegible] [illegible]Z, $CDCl_3$) δ 150.7, 148.9, 147.1, 138.8, 127.1, 127.0, 125.1, 123.5, 119.0, 115.1, 113.0, 112.8, 108.5, 69.2, 69.1, 31.8, 31.8, 29.2, 29.2, 29.1, 29.1, 26.0, 26.0, 22.6, 14.1; IR (KBr, $\bar{\upsilon}$, cm^{-1}) 3479, 3385, 2910, 2214, 1605, 1524. 1142, 843.

(*Z*)-2-(4-Aminophenyl)-3-(3,4-bis(octyloxy)phenyl)acrylonitrile (6b): Yellow solid; yield: 87% (1.63 g); mp: 119-120 °C; ^{1}H NMR (400 MHz, $CDCl_3$) δ 7.62 (d, J = 2.0 Hz, 1H, H_{Ar}), 7.48 (d, J = 8.6 Hz, 2H, H_{Ar}), 7.32 (dd, J = 8.5, 2.0 Hz, 1H, H_{Ar}), 7.29 (s, 1H, =CH), 6.91 (d, J = 8.4 Hz, 1H, H_{Ar}), 6.74 (d, J = 8.6 Hz, 2H, H_{Ar}), 4.12 – 4.05 (m, 4H, 2xO-$CH_{2\ Alkoxy}$), 3.88 (brs, 2H, NH_2), 1.91 – 1.83 (m, 4H, 2xO-β-$CH_{2\ Alkoxy}$), 1.54 – 1.47 (m, 4H, 2x$CH_{2\ Alkoxy}$), 1.24 – 1.39 (m, 16H, 2x$CH_{2\ Alkoxy}$), 0.96 – 0.87 (m, 6H, 2xMe_{Alkoxy}); ^{13}C NMR (100 MHz, $CDCl_3$) δ 150.7, 148.9, 147.1, 138.8, 127.1, 127.0, 125.1, 123.5, 119.0, 115.1, 113.0, 112.9, 108.5, 69.2, 69.1, 31.8, 29.4, 29.4, 29.3, 29.3, 29.2, 29.2, 26.1, 26.0, 22.7, 14.1; IR (KBr, $\bar{\upsilon}$, cm^{-1}) 3479, 3387, 2924, 2854, 2214, 1584, 1520, 1142, 833.

(*Z*)-2-(4-Aminophenyl)-3-(3,4-bis(dodecyloxy)phenyl)acrylonitrile (6c): Yellow solid; yield: 80% (1.53 g); mp: 90-91 °C; ^{1}H NMR (400 MHz, $CDCl_3$) 7.62 (d, J = 2.1 Hz, 1H, H_{Ar}), 7.48 (d, J = 8.6 Hz, 2H, H_{Ar}), 7.32 (dd, J = 8.5, 2.2 Hz, 1H, H_{Ar}), 7.29 (s, 1H), 6.91 (d, J = 8.4 Hz, 1H, H_{Ar}), 6.74 (d, J = 8.6 Hz, 2H, H_{Ar}), 4.14 – 4.03 (m, 4H, 2xO-$CH_{2\ Alkoxy}$), 3.88 (brs, 2H, NH_2), 1.92 – 1.82 (m, 4H, 2xO-β-$CH_{2\ Alkoxy}$), 1.56 – 1.46 (m, 4H, 2x$CH_{2\ Alkoxy}$), 1.42 – 1.29 (m, 32H, 2x$CH_{2\ Alkoxy}$), 0.92 – 0.85 (m, 6H, 2xMe_{Alkoxy}); ^{13}C NMR (100 MHz, $CDCl_3$) δ 150.7, 148.9, 147.1, 138.8, 127.1, 127.0, 125.1, 123.5, 119.0, 115.1, 113.0, 112.9, 108.5, 69.2, 69.1, 32.0, 29.7, 29.7, 29.7, 29.7, 29.7, 29.4, 29.4, 29.2, 29.2, 26.1, 26.0, 22.7, 14.2; IR (KBr, $\bar{\upsilon}$, cm^{-1}) 3476, 3387, 2913, 2847, 2206, 1605, 1520, 1143, 843.

(*Z*)-2-(4-Aminophenyl)-3-(3,4-bis(octadecyloxy)phenyl)acrylonitrile (6d): Yellow solid; yield: 85% (1.64 g); mp: 93-94 °C; ^{1}H NMR (400 MHz, $CDCl_3$) δ 7.62 (d, J = 2.1 Hz, 1H, H_{Ar}), 7.48 (d, J = 8.6 Hz, 2H, H_{Ar}), 7.32 (dd, J = 8.5, 2.0 Hz, 1H, H_{Ar}), 7.29 (s, 1H, =CH), 6.91 (d, J = 8.4 Hz, 1H, H_{Ar}), 6.74 (d, J = 8.7 Hz, 2H, H_{Ar}), 4.12 – 4.05 (m, 4H, 2xO-$CH_{2\ Alkoxy}$), 3.88 (brs, 2H, NH_2), 1.90 – 1.83 (m, 4H, 2xO-β-$CH_{2\ Alkoxy}$), 1.56 –1.46 (m, 4H, 2x$CH_{2\ Alkoxy}$), 1.40 – 1.16 (m, 56H, 2x$CH_{2\ Alkoxy}$), 0.90 – 0.85 (m, 6H, 2xMe_{Alkoxy}); ^{13}C NMR (100 MHz, $CDCl_3$) δ 150.7, 148.9, 147.1, 138.8, 127.1, 127.0, 125.1, 123.5, 119.0, 115.1, 113.0, 11.8, 108.5, 69.2, 69.1, 32.0, 29.7, 29.7, 29.7, 29.7, 29.5, 29.4, 29.4, 29.2, 29.1, 26.1, 26.01, 22.7, 14.2; IR (KBr, $\bar{\upsilon}$, cm^{-1}) 3479, 3387, 2910, 2847, 2214, 1605, 1520, 1142, 833.

General procedure for the synthesis of deoxycholic acid tethered *α*-cyanostilbenes 8a-d

To [illegible] .2 mmol) was added at 0 °C, and subsequently EDC.HCl (1.7 mmol) and HOBt (1.3 mmol) were added. The reaction mixture was stirred for 15 min. at 0 °C, after which, (*Z*)-2-(4-aminophenyl)-3-(3,4-bis(alkoxy)phenyl)acrylonitrile (**6a-d**) (1.4 mmol) was added. The reaction was stirred at room temperature for 18-24 h and its completion of the reaction was monitored by TLC. After the completion, the reaction mixture was diluted with water and extracted with DCM (3 x 20 mL). The organic layer was separated, dried over anhydrous sodium sulfate and evaporated under reduced pressure to give crude product, which was recrystallized using ethyl acetate/hexanes to yield pure **8a-d**.

(4*R*)-*N*-(4-((*Z*)-2-(3,4-Bis(heptyloxy)phenyl)-1-cyanovinyl)phenyl)-4-((3*R*,10*S*,12*S*,13*R*,17*R*)-3,12-dihydroxy-10,13-dimethylhexadecahydro-1*H*-cyclopenta[*a*]phenanthren-17-yl)pentanamide (8a): Yellow solid; yield: 84% (2.29 g); mp: 130-131 °C; ^{1}H NMR (400 MHz, $CDCl_3$) δ 7.98 (s, 1H, NH_{Amide}), 7.68 – 7.63 (m, 3H), 7.62 – 7.57 (m, 2H), 7.39 (s, 1H), 7.35 (dd, J = 8.5, 1.8 Hz, 1H), 6.91 (d, J = 8.5 Hz, 1H), 4.12 – 4.04 (m, 4H, 2xO-$CH_{2\ Alkoxy}$), 4.02 – 3.99 (m, 1H, H-12_{DCA}), 3.68 – 3.60 (m, 1H, H-3_{DCA}), 2.49 – 2.10 (m, 6H), 2.03 – 1.77 (m, 12H), 1.74 – 1.46 (m, 12H), 1.42 – 1.27 (m, 16H), 1.02 (d, J = 5.8 Hz, 3H, Me-19_{DCA}), 0.94 – 0.87 (m, 9H, Me-21_{DCA}& 2xMe_{Alkoxy}), 0.70 (s, 3H, Me-18_{DCA}); ^{13}C NMR (100 MHz, $CDCl_3$) δ 172.3 (C=O), 151.2, 148.9, 141.3, 138.8, 130.3, 126.6, 126.3, 124.0, 119.9, 48.7, 113.0, 112.7, 107.6, 73.3 (C-12_{DCA}), 71.8 (C-3_{DCA}), 69.2 (O-$CH_{2\ Alkoxy}$), 69.0 (O-$CH_{2\ Alkoxy}$), 48.2, 46.8, 46.5, 42.1, 36.4, 36.0, 35.3, 35.1, 34.2, 34.1, 34.1, 33.7, 31.8, 31.8, 31.2, 30.5, 29.2, 29.1, 29.1, 28.6, 27.6, 27.2, 26.2, 26.0, 26.0, 23.7, 23.2, 22.6 (C-19_{DCA}), 17.5 (C-21_{DCA}), 14.1 (2x$CH_{3\ Alkoxy}$), 12.8 (C-18_{DCA}); HRMS (ESI): *m/z* $[M+H]^+$ calcd for Chemical Formula: $C_{53}H_{79}N_2O_5^+$ 823.5984 found : 823.6009; $[\alpha]^{20}_D$ = +21 (*c* 1.0, MeOH); IR (KBr, $\bar{\upsilon}$, cm^{-1}) 3433, 3294, 2924, 2862, 2206, 1666, 1594, 1034, 841.

(4*R*)-*N*-(4-((*Z*)-2-(3,4-Bis(octyloxy)phenyl)-1-cyanovinyl)phenyl)-4-((3*R*,10*S*,12*S*,13*R*,17*R*)-3,12-dihydroxy-10,13-dimethylhexadecahydro-1*H*-cyclopenta[*a*]phenanthren-17-yl)pentanamide (8b): Yellow solid; yield: 82% (2.19 g); mp: 128-129 °C; ^{1}H NMR (400 MHz, DMSO-d_6) δ 10.09 (s, 1H, NH_{Amide}), 7.81 (s, 1H), 7.71 (d, J = 8.4 Hz, 2H), 7.68 – 7.60 (m, 3H), 7.48 (d, J = 7.9 Hz, 1H), 7.07 (d, J = 8.4 Hz, 1H), 4.53 – 4.47 (m, 1H, OH_{DCA}), 4.25 – 4.20 (m, 1H, H-12_{DCA}), 4.04 – 3.94(m, 4H, 2xO-$CH_{2\ Alkoxy}$), 3.80 (brs, 1H, OH_{DCA}), 3.35 – 3.32 (m, 1H, H-3_{DCA}), 2.39 – 1.89 (m, 4H), 1.87 – 1.64 (m, 12H), 1.58 – 1.35 (m, 12H), 1.32 – 1.10 (m, 22H), 0.97 (d, J = 5.0 Hz, 3H, Me-19_{DCA}), 0.90 – 0.79 (m, 9H, Me-21_{DCA} & 2xMe_{Alkoxy}), 0.60 (s, 3H, Me-18_{DCA}); ^{13}C NMR (100 MHz, DMSO-d_6) δ 172.4 (C=O), 151.1, 148.6, 141.5, 140.4, 128.9, 126.9, 126.3, 124.0, 119.6, 119.0, 114.0, 113.5, 107.0, 71.5 (C-12_{DCA}), 70.4 (C-3_{DCA}), 68.8 (O-

Cl[illegible]4, 31.7, 30.7, 29.2, 29.1, 27.7, 27.4, 26.6, 26.1, 24.0, 23.5, 23.3, 22.6 (C-19_{DCA}), 17.6 (C-21_{DCA}), 14.4 (2x$CH_{3\ Alkoxy}$), 12.9 (C-18_{DCA}); HRMS (ESI): *m/z* $[M+Na]^+$ calcd for Chemical Formula: $C_{55}H_{82}N_2O_5Na^+$ 873.6116 found : 873.6173; $[\alpha]^{20}_D$ = +92 (*c* 1.0, MeOH); IR (KBr, $\bar{\upsilon}$, cm^{-1}) 3502, 3294, 3178, 2924, 2854, 2206, 1666, 1597, 1041, 841.

(4*R*)-*N*-(4-((*Z*)-2-(3,4-bis(dodecyloxy)phenyl)-1-cyanovinyl)phenyl)-4-((3*R*,10*S*,12*S*,13*R*,17*R*)-3,12-dihydroxy-10,13-dimethylhexadecahydro-1*H*-cyclopenta[*a*]phenanthren-17-yl)pentanamide (8c): Yellow solid; yield: 85% (1.38 g); mp: 140-141 °C; ^{1}H NMR (400 MHz, DMSO-d_6 + $CDCl_3$) δ 10.02 (s, 1H, NH_{Amide}), 7.75 – 7.68 (m, 3H), 7.66 – 7.58 (m, 3H), 7.45 (d, *J* = 7.8 Hz, 1H), 7.00 (d, *J* = 8.6 Hz, 1H), 4.48 – 4.42 (m, 1H, OH_{DCA}), 4.18 – 4.15 (m, 1H, H-12_{DCA}), 4.03 – 3.95 (m, 4H, 2xO-$CH_{2\ Alkoxy}$), 3.80 (brs, 1H, OH_{DCA}), 3.36 – 3.33 (m, 1H, H-3_{DCA}), 2.38 – 2.05 (m, 4H), 1.99 – 1.51 (m, 22H),1.41 – 1.32 (m, 10H), 1.28 – 1.22 (m, 30H), 0.98 (d, *J* = 5.8 Hz, 3H, Me-19_{DCA}), 0.88 – 0.80 (m, 9H, Me-21_{DCA}& 2xMe_{Alkoxy}), 0.60 (s, 3H, Me-18_{DCA}); ^{13}C NMR (100 MHz, DMSO-d_6 + $CDCl_3$) δ 172.4 (C=O), 151.1, 148.7, 141.2, 140.4, 129.0, 126.9, 126.2, 124.1, 119.6, 118.9, 113.9, 113.4, 107.2, 71.6 (C-12_{DCA}), 70.5 (C-3_{DCA}), 68.9 (O-$CH_{2\ Alkoxy}$), 68.7 (O-$CH_{2\ Alkoxy}$), 47.9, 46.6, 46.4, 42.1, 36.7, 36.1, 35.6, 35.6, 35.3, 34.3, 33.9, 33.4, 31.9, 30.1, 29.7, 29.6, 29.6, 29.6, 29.3, 29.3, 29.2, 29.2, 29.1, 29.0, 27.7, 27.5, 26.5, 26.1, 24.0, 23.5, 23.3, 22.6 (C-19_{DCA}), 17.6 (C-21_{DCA}), 14.4 (2x$CH_{3\ Alkoxy}$), 12.9 (C-18_{DCA}); HRMS (ESI): *m/z* $[M+H]^+$ calcd for Chemical Formula: $C_{63}H_{99}N_2O_5^+$ 963.7549 found : 963.7585; $[\alpha]^{20}_D$ = +13 (*c* 1.0, MeOH); IR (KBr, $\bar{\upsilon}$, cm^{-1}) 3502, 3294, 2924, 2854, 2206, 1659, 1597, 1041, 841.

(4*R*)-*N*-(4-((*Z*)-2-(3,4-Bis(octadecyloxy)phenyl)-1-cyanovinyl)phenyl)-4-((3*R*,10*S*,12*S*,13*R*,17*R*)-3,12-dihydroxy-10,13-dimethylhexadecahydro-1*H*-cyclopenta[*a*]phenanthren-17-yl)pentanamide (8d): Yellow solid; yield: 81% (1.82 g); mp: 138-139 °C; ^{1}H NMR (400 MHz, $CDCl_3$) δ 7.62 (dd, *J* = 8.6, 2.3 Hz, 1H), 7.52 (d, *J* = 2.4 Hz, 1H), 7.39 – 7.35 (m, 2H), 7.19 (s, 1H), 7.16 (s, 1H), 6.90 (d, *J* = 8.6 Hz, 1H), 6.66 – 6.62 (m, 2H), 3.98 – 3.91 (m, 4H, 2xO-$CH_{2\ Alkoxy}$), 3.84 – 3.74 (m, 1H, H-12_{DCA}), 3.58 – 3.50 (m, 1H, H-3_{DCA}), 2.66 – 2.52 (m, 2H), 2.50 – 2.34 (m, 2H), 1.94 – 1.56 (m, 22H), 1.52 – 1.32 (m, 20H), 1.28 – 1.14 (m, 44H), 0.98 (d, *J* = 5.7 Hz, 3H, Me-19_{DCA}), 0.88 – 0.78 (m, 9H, Me-21DCA & 2xMe_{Alkoxy}), 0.64 (s, 3H, Me-18_{DCA}); ^{13}C NMR (100 MHz, $CDCl_3$) δ 172.0 (C=O), 152.0, 147.3, 140.1, 137.4, 128.2, 127.1, 127.0, 124.8, 118.5, 115.1, 113.1, 109.5, 73.2 (C-12_{DCA}), 71.9 (C-3_{DCA}), 68.8 (O-$CH_{2\ Alkoxy}$), 48.3, 47.4, 46.6, 42.1, 36.5, 36.1, 35.2, 35.1, 34.1, 33.7, 31.9, 30.9, 30.5, 29.7, 29.7, 29.7, 29.7, 29.4, 29.4, 29.1, 28.7, 27.5, 7.1, 26.2, 25.9, 23.7, 23.2, 22.7 (C-19_{DCA}), 17.4 (C-21_{DCA}), 14.1 ($_{2xCH3\ Alkoxy}$), 12.8 (C-18_{DCA}); HRMS (ESI): *m/z* $[M+Na]^+$ calcd for Chemical

Fo[illegible] $\bar{\upsilon}$, cm^{-1}) 3433, 3294, 2924, 2862, 2206, 1666, 1594, 1034, 841.

Procedure for gelation for compounds 8a-d

In a screw cap vial, gelator (10 mg-20 mg) was added in a solvent (1 mL) and heated or swirled in an oil bath until all the solid was completely dissolved. In most of the solvents, all gelators becomes soluble at room temperature upon gentle swirling and heating was not required. The vials were left undisturbed at room temperature. The gelation (G) was confirmed when no flow was observed after inversion of the vial, if the formed gel was stable at lower temperature (>20˚C) but unstable at room temperature (20˚C) it was confirmed as weak gel (WG), if the gelator was partially soluble at room temperature it was confirmed as partial soluble (PS), if a clear solution (>70 mg) was obtained the state was marked as soluble (S). Some formed gels were found to be transparent while others were found to be opaque. The minimum gelation concentration (MGC) was determined by measuring the minimum amount of gelator required for the formation of the gel at room temperature.[50]

Scanning Electron Microscopy Analysis (SEM)

Morphology of the freeze dried gels were determined using Scanning Electron Microscope (SEM) from Carl Zeiss (Σigma VP). The powder samples were spread over the carbon tape and coated with Au-Pd alloy for 2 min. The gel sample was spread over a silicon wafer and dried completely followed by coating with Au-Pd alloy for 2 min. Gels were dried using a labcon lyophillizer.

Transmission Electron Microscopy Analysis (TEM)

The TEM analysis were performed by placing a small amount of gel in xylene and toluene at MGC on the copper grid and dried at room temperature for 24 h. Images were taken on JEOL-2010F TEM operating with electron beam of energy of 200 kV.

FT-IR Analysis

FT-IR was taken on ABB Bomen MB 3000 FTIR for gelator and freeze dried gels, using KBr disk technique.

XRD Analysis

XRD analysis of the xerogel was recorded on the Rigaku Ultima IV fully automatic high resolution X-ray diffractometer system with Theta-Theta (θ-θ) Goniometer.

Fluorescence Microscopic Study

A small amount of gel obtained from respective solvents at minimum gel concentration was placed on a glass coverslip slide and was kept undisturbed under dust free environment for slow evaporation of the solvent and finally dried under vaccum to obtain xerogel which was placed

filter using 100X objective lens and 10 X eyepiece lens.

Procedure for bio-imaging

The compounds were tested for its bio-imaging application against the gram –ve bacterium *Serratia marcescens* and gram +ve bacterium *Staphylococcus aureus*. The bacterial strain were cultured using Luria-Bertani medium (Hi-media, India) at 37 °C on a rotary shaker with 150 rpm. The fluorescent staining was performed using the previously described procedure with slight modifications (Moyes, 2009). The bacterial cultures were grown up to mid-log phase and incubated with 50 μg/mL concentration of compounds at 37 °C for 30 min. Following incubation, 5 μL of each bacterial culture was used for preparing the smears on the glass slide. The smears were fixed using the 95% ethanol for 5 min and washed by 1 X PBS buffer (Phosphate buffer saline, pH 7.2). The smears were air-dried and covered with glass cover-slips. The fluorescent images of bacteria was captured using the epi-Fluorescence Microscope (Olympus-BX41, Olympus, Japan) at 100X objective lens and 10 X eyepiece lens.

Conflicts of interest

There are no conflicts to declare.

Acknowledgements

The author RS would like to acknowledge UGC and BITS Pilani for research funding. The author DA is thankful to BITS Pilani, for providing fellowship. We also like to thank central NMR facility, BITS Pilani and financial support from DST under FIST program [Project: SR/FST/CSI-270/2015] for HRMS facility. The authors would also like to thank Materials Research Centre (MRC), MNIT, Jaipur for TEM analysis.

References

[1] A.K. Vasu, M. Radhakrishna, S. Kanvah, Self-Assembly Tuning of α-Cyanostilbene Fluorogens: Aggregates to Nanostructures, J. Phys. Chem. C 121(40) (2017) 22478-22486.

[2] V. Palakollu, S. Kanvah, Cholesterol-tethered AIEE fluorogens: formation of self-assembled nanostructures, RSC Adv. 5(42) (2015) 33049-33057.

[3] W. Zhang, Y. Chris, R.T. Kwok, J.W. Lam, B.Z. Tang, A photostable AIE luminogen with near infrared emission for monitoring morphological change of plasma membrane, J. Mater. Chem. B 6(10) (2018) 1501-1507.

[4] E. Kim, Y. Lee, S. Lee, S.B. Park, Discovery, understanding, and bioapplication of organic fluorophore: a case study with an indolizine-based novel fluorophore, Seoul-Fluor, Acc. Chem. Res. 48(3) (2015) 538-547.

[5] nd biological applications, Acc. Chem. Res. 50(2) (2017) 366-375.

[6] Y. Li, T. Liu, H. Liu, M.-Z. Tian, Y. Li, Self-assembly of intramolecular charge-transfer compounds into functional molecular systems, Acc. Chem. Res. 47(4) (2014) 1186-1198.

[7] J. Katla, A.J. Nair, A. Ojha, S. Kanvah, Organogels composed of trifluoromethyl anthryl cyanostyrenes: enhanced emission and self-assembly, Photochem. Photobiol. Sci. 17(4) (2018) 395-403.

[8] Y. Ma, M. Cametti, Z. Džolić, S. Jiang, Responsive aggregation-induced emissive supramolecular gels based on bis-cyanostilbene derivatives, J. Mater. Chem. C 4(46) (2016) 10786-10790.

[9] X. Wang, Z. Ding, Y. Ma, Y. Zhang, H. Shang, S. Jiang, Multi-stimuli responsive supramolecular gels based on a D–π–A structural cyanostilbene derivative with aggregation induced emission properties, Soft matter 15(7) (2019) 1658-1665.

[10] D. Ding, K. Li, B. Liu, B.Z. Tang, Bioprobes based on AIE fluorogens, Acc. Chem. Res. 46(11) (2013) 2441-2453.

[11] A. Ravikrishnan, P. Sudhakara, P. Kannan, Stilbene-based liquid crystalline and photocrosslinkable polynaphthylphosphate esters, J. Mater. Sci. 45(2) (2010) 435-442.

[12] J. Mei, N.L. Leung, R.T. Kwok, J.W. Lam, B.Z. Tang, Aggregation-induced emission: together we shine, united we soar!, Chem. Rev. 115(21) (2015) 11718-11940.

[13] B.-K. An, D.-S. Lee, J.-S. Lee, Y.-S. Park, H.-S. Song, S.Y. Park, Strongly fluorescent organogel system comprising fibrillar self-assembly of a trifluoromethyl-based cyanostilbene derivative, J. Am. Chem. Soc. 126(33) (2004) 10232-10233.

[14] B.-K. An, J. Gierschner, S.Y. Park, π-Conjugated cyanostilbene derivatives: a unique self-assembly motif for molecular nanostructures with enhanced emission and transport, Acc. Chem. Res. 45(4) (2011) 544-554.

[15] S.J. Yoon, S. Varghese, S.K. Park, R. Wannemacher, J. Gierschner, S.Y. Park, Color-Tuned, Highly Emissive Dicyanodistyrylbenzene Single Crystals: Manipulating Intermolecular Stacking Interactions for Spontaneous and Stimulated Emission Characteristics, Adv. Opt. Mater. 1(3) (2013) 232-237.

[16] B.-K. An, S.H. Gihm, J.W. Chung, C.R. Park, S.-K. Kwon, S.Y. Park, Color-tuned highly fluorescent organic nanowires/nanofabrics: easy massive fabrication and molecular structural origin, J. Am. Chem. Soc. 131(11) (2009) 3950-3957.

[17] F.t. Aparicio, S. Cherumukkil, A. Ajayaghosh, L. Sánchez, Color-tunable cyano-substituted divinylene arene luminogens as fluorescent π-gelators, Langmuir 32(1) (2015) 284-289.

[18] Y. Chen, J.W. Lam, R.T. Kwok, B. Liu, B.Z. Tang, Aggregation-induced emission: fundamental understanding and future developments, Mater. Horiz. 6(3) (2019) 428-433.

[1] [illegible] to the field of biomedicine, ACS Appl. Bio Mater. 1(6) (2018) 1768-1786.

[20] S. Kagatikar, D. Sunil, Aggregation-induced emission of azines: An up-to-date review, J. Mol. Liq. (2019) 111371.

[21] E.R. Jimenez, H. Rodríguez, Aggregation-induced emission: a review of promising cyano-functionalized AIEgens, J. Mater. Sci. (2020) 1-22.

[22] B. Liu, B.Z. Tang, Themed Issue on Aggregation-Induced Emission (AIE), Chem. Asian J. 14(6) (2019) 672-673.

[23] X. Li, M. Jiang, J.W. Lam, B.Z. Tang, J.Y. Qu, Mitochondrial imaging with combined fluorescence and stimulated Raman scattering microscopy using a probe of the aggregation-induced emission characteristic, J. Am. Chem. Soc. 139(47) (2017) 17022-17030.

[24] X. Zhang, X. Huang, X. Gan, Z. Wu, J. Yu, H. Zhou, Y. Tian, J. Wu, Two multi-functional aggregation-induced emission probes: reversible mechanochromism and bio-imaging, Sens. Actuators, B 243 (2017) 421-428.

[25] S. Dhoun, S. Kaur, P. Kaur, K. Singh, A cyanostilbene-boronate based AIEE probe for hydrogen peroxide—Application in chemical processing, Sens. Actuators, B 245 (2017) 95-103.

[26] G. Zhang, X. Zhang, Y. Zhang, H. Wang, L. Kong, Y. Tian, X. Tao, H. Bi, J. Yang, Design of turn-on fluorescent probe for effective detection of Hg2+ by combination of AIEE-active fluorophore and binding site, Sens. Actuators, B 221 (2015) 730-739.

[27] J.W. Chung, B.-K. An, S.Y. Park, A thermoreversible and proton-induced gel− sol phase transition with remarkable fluorescence variation, Chem. Mater. 20(21) (2008) 6750-6755.

[28] S. Guo, J. Pan, J. Huang, L. Kong, J. Yang, Two AIEE-active α-cyanostilbene derivatives containing BF 2 unit for detecting explosive picric acid in aqueous medium, RSC Adv. 9(45) (2019) 26043-26050.

[29] Y. Zhang, J. Huang, L. Kong, Y. Tian, J. Yang, Two novel AIEE-active imidazole/α-cyanostilbene derivatives: photophysical properties, reversible fluorescence switching, and detection of explosives, CrystEngComm 20(9) (2018) 1237-1244.

[30] P. Xing, H. Chen, L. Bai, Y. Zhao, Photo-triggered transformation from vesicles to branched nanotubes fabricated by a cholesterol-appended cyanostilbene, Chem. Commun. 51(45) (2015) 9309-9312.

[31] Y. Zhang, Y. Ma, M. Deng, H. Shang, C. Liang, S. Jiang, An efficient phase-selective gelator for aromatic solvents recovery based on a cyanostilbene amide derivative, Soft matter 11(25) (2015) 5095-5100.

[3] ve gelator for aromatic solvents recovery based on a cyanostilbene amide derivative, Soft matter 11(30) (2015) 6162-6162.

[33] M. Zhang, S. Strandman, K.C. Waldron, X. Zhu, Supramolecular hydrogelation with bile acid derivatives: structures, properties and applications, J. Mater. Chem. B 4(47) (2016) 7506-7520.

[34] P. Babu, N.M. Sangeetha, U. Maitra, Supramolecular chemistry of bile acid derivatives: formation of gels, Macromolecular Symposia, Wiley Online Library, 2006, pp. 60-67.

[35] Z. Helan, P. Junxia, L. Kaiqiang, F. Yu, Supramolecular Gels of Cholic Acids and Their Derivatives, Prog. Chem. 23(8) (2011) 1591-1597.

[36] U. Maitra, A. Chakrabarty, Protonation and deprotonation induced organo/hydrogelation: Bile acid derived gelators containing a basic side chain, Beilstein J. Org. Chem. 7(1) (2011) 304-309.

[37] S. Mukhopadhyay, U. Maitra, Chemistry and biology of bile acids, Curr. Sci. 87(12) (2004) 1666-1683.

[38] N.M. Sangeetha, U. Maitra, Supramolecular gels: Functions and uses, Chem. Soc. Rev. 34(10) (2005) 821-836.

[39] N.F. Goldshleger, A.S. Lobach, V.E. Baulin, A.Y. Tsivadze, Supramolecular gels based on bile acid salts, Russ. Chem. Rev. 86(4) (2017) 269.

[40] D.S. Agarwal, N. Gogoi, D. Chowdhury, R. Sakhuja, Amino acid appended cholic acid–azobenzene dyad: an effective & smart phase selective gelator for aromatic solvents, RSC Adv. 6(80) (2016) 76632-76641.

[41] N. Gogoi, D.S. Agarwal, A. Sehgal, D. Chowdhury, R. Sakhuja, One-Pot Synthesis of Carbon Nanodots in an Organic Medium with Aggregation-Induced Emission Enhancement (AIEE): A Rationale for “Enzyme-Free” Detection of Cholesterol, ACS Omega 2(7) (2017) 3816-3827.

[42] D.S. Sarma, A. Palanisamy, Self-assembly of aromatic biscarbamate gelators: effect of spacer length on the gelation and rheology, J. Sol-Gel Sci. Technol. 79(3) (2016) 637-649.

[43] U. Maitra, M. Maity, Supramolecular gels from Bile acid-Amino acid conjugates and their Applications, Eur. J. Org. Chem (2017) 1713-1720.

[44] K. Basu, N. Nandi, B. Mondal, A. Dehsorkhi, I.W. Hamley, A. Banerjee, Peptide-based ambidextrous bifunctional gelator: applications in oil spill recovery and removal of toxic organic dyes for waste water management, Interface Focus 7(6) (2017) 20160128.

[45] D.R. Trivedi, A. Ballabh, P. Dastidar, Facile preparation and structure–property correlation of low molecular mass organic gelators derived from simple organic salts, Journal of Materials Chemistry 15(26) (2005) 2606-2614.

[4] ne arrays of side chain modified bile acids derivatives. Two novel self-assemblies based on π-π and belly-to-belly interactions, Steroids 115 (2016) 169-176.

[47] V.C. Edelsztein, A.S. Mac Cormack, M. Ciarlantini, P.H. Di Chenna, Self-assembly of 2, 3-dihydroxycholestane steroids into supramolecular organogels as a soft template for the in-situ generation of silicate nanomaterials, Beilstein J. Org. Chem. 9(1) (2013) 1826-1836.

[48] R. Kuosmanen, R. Puttreddy, K. Rissanen, E. Sievänen, Systematic Modulation of the Supramolecular Gelation Properties of Bile Acid Alkyl Amides, Chem. Eur. J. 24(70) (2018) 18676-18681.

[49] M. Löfman, J. Koivukorpi, V. Noponen, H. Salo, E. Sievänen, Bile acid alkylamide derivatives as low molecular weight organogelators: Systematic gelation studies and qualitative structural analysis of the systems, J. Colloid Interface Sci. 360(2) (2011) 633-644.

[50] A.R. Katritzky, R. Sakhuja, L. Khelashvili, K. Shanab, Gelation Behavior of 2 H-Chromene N-Acylamino Acid Conjugates, J. Org. Chem. 74(8) (2009) 3062-3065.

Highlights

- Four novel deoxycholic acid tethered *α*-cyanostilbenes were synthesized and characterized.
- The synthesized deoxycholic acid tethered *α*-cyanostilbene derivatives formed stable gels with a variety of solvents.
- The stable gels showed lamellar sheet type structures stacked over each other, consisting of entangled fibres.
- The synthesized compounds also exhibited AIEE behaviour in H_2O/THF mixture and the AIEE property was explored for bacterial bio-imaging.